

# False vacuum decay in an ultracold spin-1 Bose gas

Thomas P. Billam,<sup>1,\*</sup> Kate Brown,<sup>2,†</sup> and Ian G. Moss<sup>2,‡</sup>

<sup>1</sup>*Joint Quantum Centre (JQC) Durham–Newcastle, School of Mathematics,  
Statistics and Physics, Newcastle University, Newcastle upon Tyne, NE1 7RU, UK*

<sup>2</sup>*School of Mathematics, Statistics and Physics, Newcastle University, Newcastle upon Tyne, NE1 7RU, UK*  
(Dated: February 11, 2022)

We propose an ultracold atom analogue of false vacuum decay using all three states of a spin-1 Bose gas. We consider a one-dimensional system with both radio frequency and optical Raman coupling between internal states. An advantage of our proposal is the lack of a time-modulated coupling, which can lead to instabilities. Within the elaborate phase structure of the system we identify an effective Klein-Gordon field and use Gross-Pitaevskii simulations within the truncated Wigner approximation to model the decay of a metastable state. We examine the dependence of the rate of vacuum decay on particle density for <sup>7</sup>Li and <sup>41</sup>K and find reasonable agreement with instanton methods.

First-order phase transitions, characterised by metastable, supercooled states and the nucleation of bubbles, form an important class of physical phenomena. In extreme cases, supercooling can lead to a zero-temperature, ‘false vacuum’ state, and the subsequent decay of the false vacuum via quantum tunnelling [1–3].

The non-perturbative description of vacuum decay involves an *instanton*, or *bounce*, solution to the field equations in imaginary time [1–3]. However, the instanton approach gives limited information about how the bubbles emerge in real-time, and how bubble nucleation events are correlated. A recent suggestion has been to explore the details of false vacuum decay in ultracold atom systems, where the impressive degree of experimental control available raises the possibility of engineering (possibly quasi-relativistic) false vacua. The scheme of Fialko et al. [4, 5] is one such proposal. This uses a two-component Bose gas in one dimension formed from two spin states of a spinor condensate, coupled by a time-modulated microwave field. After time-averaging, one obtains an effective description containing a metastable false vacuum state in addition to the true vacuum ground state.

Refs. [4–8] studied the decay of the false vacuum using field-theoretical instanton techniques and numerical simulations based on the truncated Wigner methodology [9, 10]. However, Refs. [6, 11] showed that the false vacuum state in this scheme can suffer from a parametric instability caused by the time-modulation of the system. The instability causes decay of the false vacuum state by a different mechanism than a first-order phase transition. This instability presents a challenge to experimental implementation of the scheme [6, 11, 12]. Furthermore, the scheme requires inter-component interactions to be small compared to intra-component interactions; this necessitates working close to a Feshbach resonance [4, 5], which limits flexibility in the experimental setup.

Clearly, it would be desirable to have an ultracold atom system that simulates vacuum decay while being free of the need to time-modulate the microwave field and, ideally, more flexible in terms of experimental setup. In this Letter we show that this can be achieved using a spin-1 Bose Einstein condensate system with external coupling fields. By careful choice of couplings, the system we propose undergoes vacuum decay in

a way that is analogous to a Klein-Gordon system.

We will describe the system in one dimension (1D), assuming the atoms to be tightly harmonically confined in the transverse directions such that a quasi-1D description is suitable. The description generalises to two or three dimensions. We consider a condensate of alkali atoms in their  $F = 1$  hyperfine ground state manifold. The degeneracy between internal spin states  $|m\rangle$ , where  $m \in \{-1, 0, 1\}$ , is lifted by a static magnetic field  $B_z$  along the  $z$  axis. In addition to intrinsic collisional coupling between the spin states, described by a quartic Hamiltonian, we propose the states be extrinsically coupled by both radio frequency fields (RF coupling) and by optical fields in a two-photon Raman scheme (Raman coupling).

The quadratic terms in our mean field Hamiltonian are

$$H_2 = \int dx \left\{ \bar{\psi} \left[ \frac{-\hbar^2 \nabla^2}{2m} - \mu \right] \psi + \bar{\psi} H_B^{ZE} \psi + \bar{\psi} H_B^{MIX} \psi \right\}, \quad (1)$$

where the field  $\psi$  has components  $\psi_m$ . The constant magnetic field produces a first order Zeeman effect with frequency  $\omega_z = g_F \mu_B B_z / \hbar$  and a second order Zeeman effect with frequency  $\omega_q$ ,

$$H_B^{ZE} = \hbar \omega_z J_z + \hbar \omega_q J_z^2, \quad (2)$$

where  $J_x$ ,  $J_y$  and  $J_z$  are the dimensionless angular momentum generators. The RF field has frequency  $\omega_z$  and is polarised in the  $x$  direction. This directly couples states with azimuthal quantum numbers  $m \leftrightarrow m \pm 1$ . Coupling of the  $m \leftrightarrow m \pm 2$  states can be achieved by two optical fields arranged on the  $D_1$  line, creating a two-photon Raman coupling between the states in a three-level  $\Lambda$  scheme, as shown in Fig. 1. In presenting our system we neglect complications arising from other states in the upper hyperfine manifold, and consider only a single excited state  $|e\rangle$  with azimuthal quantum number zero. To avoid population of  $|e\rangle$ , the detuning  $\Delta$  should be large compared to relevant atomic linewidths, and to keep the momentum transferred to the atoms negligible the optical fields driving  $\sigma_{\pm}$  transitions should be co-propagating

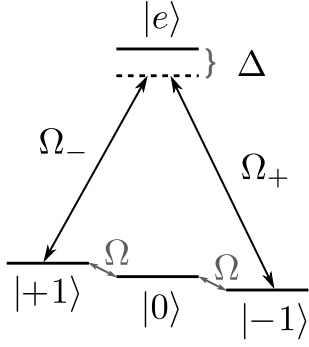


FIG. 1. Level coupling diagram for the simplest  $\Lambda$  system based on Raman and microwave induced transitions. The  $F = 1$  spin states labelled  $|m\rangle$ , are coupled by a resonant RF beam of frequency  $\omega_z$ , with Rabi frequency  $\Omega$ , and by a two-photon Raman coupling induced by off-resonant optical beams with Rabi frequencies  $\Omega_{\pm}$ , zero two-photon detuning, and detuning  $\Delta$  from the excited state  $|e\rangle$ .

in the  $z$ -direction [13]. We assume zero two-photon detuning. After time-averaging of the RF and optical frequencies in the rotating wave approximation, we obtain the mixing part of the Hamiltonian

$$H_B^{MIX} = \frac{1}{2}\hbar\Omega J_x + \frac{1}{2}\hbar\alpha (J_+^2 + J_-^2), \quad (3)$$

where the frequency  $\Omega = g_F\mu_B B_x/\hbar$  depends on the RF field amplitude  $B_x$ , and  $\alpha = -\Omega_+\Omega_-/4\Delta$  is determined by the optical-field Rabi frequencies  $\Omega_{\pm}$  and the detuning  $\Delta$ .

We assume that the atomic collisions are described by rotationally invariant dipole-dipole interactions  $(\bar{\psi}\psi)^2$  and  $(\bar{\psi}\mathbf{J}\psi)^2$ , which we would expect to describe a whole range of systems with low to moderate external magnetic fields [14, 15]. The interaction terms can be gathered together into an interaction potential function  $V$ , so that the total Hamiltonian becomes

$$H = \int dx \left\{ \bar{\psi} \left[ \frac{-\hbar^2\nabla^2}{2m} \right] \psi + V(\bar{\psi}, \psi) \right\}. \quad (4)$$

where

$$V = -\mu\bar{\psi}\psi + \hbar\omega_q(\bar{\psi}J_z^2\psi) + \frac{1}{2}g(\bar{\psi}\psi)^2 + \frac{1}{2}g'(\bar{\psi}\mathbf{J}\psi)^2 + \frac{1}{2}\hbar\Omega\bar{\psi}J_x\psi + \frac{1}{2}\hbar\alpha\bar{\psi}(J_+^2 + J_-^2)\psi. \quad (5)$$

Here,  $g = 2\hbar\omega_r(a_0 + 2a_2)/3$  and  $g' = 2\hbar\omega_r(a_2 - a_0)/3$  where  $a_F$  is the  $s$ -wave scattering length for total-spin- $F$  channels [14, 15], and  $\omega_r$  is the trap frequency of the symmetric transverse confinement. Note that the linear Zeeman term is cancelled out by the RF field in the rotating wave approximation, and the magnetisation is not conserved due to mixing. The appropriate treatment of the spin-1 system for our purposes is one with a fixed chemical potential but no additional Lagrange multiplier for the magnetisation.

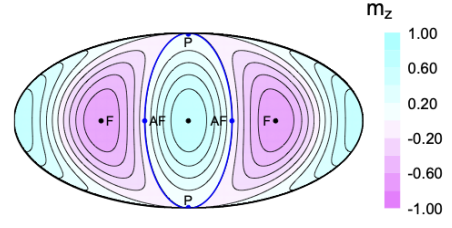


FIG. 2. Mollweide projection of the sphere  $\zeta_0^2 + \zeta_{+1}^2 + \zeta_{-1}^2 = 1$  ( $\zeta_0$  in the vertical direction) showing the ground states superimposed on contours of constant magnetisation. The blue line represents the locus of BA vacua ( $\zeta_+ = \zeta_-$ ) for different external magnetic field strengths.

The spin-1 system has a rich phase structure, even in the absence of mixing terms. Following Kawaguchi and Ueda [14], the fields can be parameterised by

$$\psi_{\pm 1} = \sqrt{\rho} \zeta_{\pm 1} e^{i(\theta \pm \varphi)}, \quad (6)$$

$$\psi_0 = \sqrt{\rho} \zeta_0, \quad (7)$$

subject to  $\zeta_0^2 + \zeta_{+1}^2 + \zeta_{-1}^2 = 1$ . The configuration space is the quadrant  $\zeta_0 > 0$ ,  $\zeta_{\pm} > 0$  of Fig. 2 and  $0 < \theta < \pi$ ,  $0 < \varphi < \pi$ . The ferromagnetic phases (F) are characterised by having magnetisation  $m_z = \zeta_+^2 - \zeta_-^2 = \pm 1$ . The other phases have zero magnetisation in our system, and they are the antiferromagnetic (AF) phase with  $\zeta_0 = 0$ , the polar (P) phase with  $\zeta_0 = 1$  and the broken axisymmetric phase (BA). These phases have been observed experimentally in  $^{87}\text{Rb}$  [16].

We will focus on the BA phase which has the lowest energy when  $g' < 0$ ,  $g > 0$  and  $0 < \hbar\omega_q < -2g'\rho$ . If the mixing terms are absent, then  $\zeta_{+1} = \zeta_{-1} = \zeta$  at the minimum, where

$$\zeta = \frac{1}{2} \left( 1 + \frac{\hbar\omega_q}{2g'\rho} \right)^{1/2}. \quad (8)$$

Furthermore, we work in the regime  $|g'/g| \ll 1$ , where  $\mu \approx g\rho$ , and also in the regime of weak mixing ( $|\hbar\Omega| \ll \mu$ ) in which the states have approximately the same moduli as above. Crucially, however, the weak mixing terms raise the degeneracy between different values of the phase so that there are stationary points when  $(\theta, \varphi)$  equals  $(0, 0)$ ,  $(\pi, 0)$ ,  $(0, \pi)$  and  $(\pi, \pi)$ . The second derivatives of the potential imply that the stationary points become local minima when  $|\hbar\Omega| \lesssim -2g'\rho$  and  $|\Omega| \lesssim -4\alpha$ , as shown in Fig. 3.

Before considering in the dynamics of the phases  $\theta$  and  $\varphi$  it proves convenient to rescale the system to natural units. The healing length  $\xi = \hbar/(mg\rho)^{1/2}$  and natural frequency  $\omega_0 = g\rho/\hbar$  are defined in the usual way. We use the healing length as the length unit,  $1/\omega_0$  as the time unit and  $g\rho$  as the energy unit. Dimensionless parameters  $\epsilon$  and  $\lambda$  describe the strength of the mixing terms,  $\epsilon^2 = \hbar\Omega/g\rho$  and  $\lambda^2 = \Omega_+\Omega_-/\Omega\Delta$ .

The Klein-Gordon mode can be isolated by fixing  $\rho$  and taking  $\zeta_{\pm} = \zeta e^{\pm i\sigma/2}$ . The potential barrier heights in the

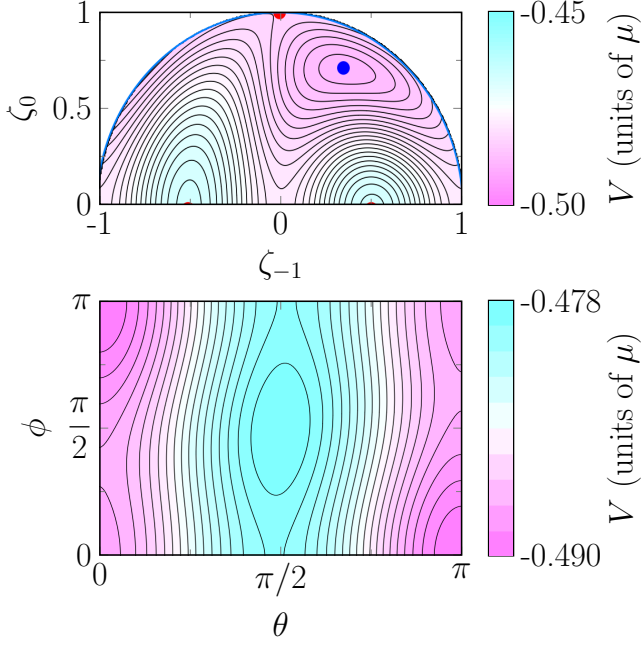


FIG. 3. The false vacuum, with RF and Raman mixing terms included, is shown in different projections of the potential  $V$  (in units of  $\mu$ ). The top figure shows the potential as function of the relative amplitudes of the spin components in a quadrant of the Mollweide projection at  $(\theta, \varphi) = (0, 0)$  and fixed  $\mu$ . The BA vacuum state is indicated by a blue dot. Below, the potential as a function of the phase angles at  $\zeta_{\pm} = \zeta$ . The false vacuum is at  $(\theta, \varphi) = (0, 0)$  and the true vacuum at  $(\pi, 0)$ . In this example,  $g' = -0.0256g$ ,  $\epsilon = 0.05$ ,  $\lambda = 1.7$  and  $\omega_q = 0.017\mu/\hbar$  (see Table I).

$\theta$  and  $\varphi$  directions depend on  $g'/g$  and  $\epsilon$  respectively. We take the case where the barrier is smaller in the  $\varphi$  directions, i.e.  $\epsilon^2 \ll |g'/g|$ . The effective Lagrangian density  $\mathcal{L}_{\text{eff}}$  at  $O(\epsilon^2)$  then describes a Klein-Gordon field  $\varphi$  with effective Lagrangian,

$$\mathcal{L}_{\text{eff}} = 2\zeta^2\rho \left\{ \frac{1}{2c^2}(\partial_t\varphi)^2 - \frac{1}{2}(\nabla\varphi)^2 - V_{\text{eff}}(\varphi) \right\}. \quad (9)$$

The propagation speed of the Klein Gordon field is  $c$ , where  $c^2 = \omega_q/2$  in healing length units. The potential  $V_{\text{eff}}(\varphi)$  is

$$V_{\text{eff}} = \epsilon^2\lambda_c^2 \cos\varphi + \frac{1}{2}\lambda^2\epsilon^2 \sin^2\varphi, \quad (10)$$

where

$$\lambda_c = \left( \frac{1 - g\omega_q/2g'}{1 + g\omega_q/2g'} \right)^{1/2}. \quad (11)$$

The potential has a true vacuum at  $\varphi = \pi$  and a false vacuum at  $\varphi = 0$  provided that  $\lambda > \lambda_c$ . The effective Klein-Gordon field has a mass  $m_\varphi = \epsilon(\lambda^2 - \lambda_c^2)^{1/2}$  in the false vacuum.

We now perform numerical simulations using the projected Gross-Pitaevskii equation (PGPE) in the truncated Wigner approximation (TWA) to examine how the decay of the false

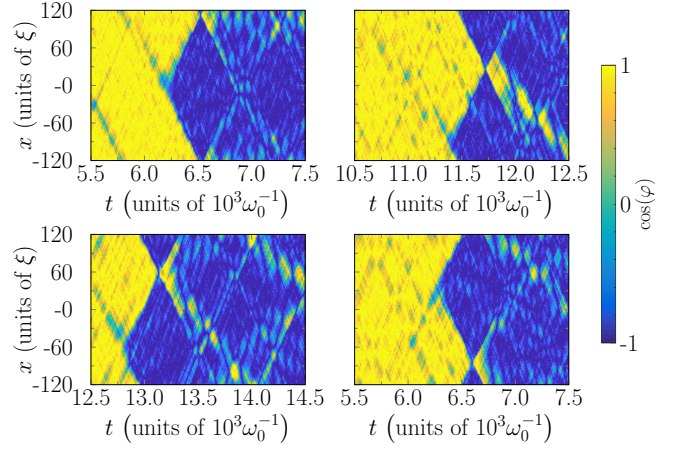


FIG. 4. Example trajectories showing bubble nucleation in  ${}^7\text{Li}$  (see Table I) with dimensionless coupling parameters  $\lambda = 1.7$  and  $\epsilon = 0.05$ , and dimensionless density  $\rho\xi = 20$ .

vacuum proceeds in the fully non-linear system. On the face of things, the existing theory behind the TWA approach does not extend to non-perturbative quantum phenomena. However, numerical simulations carried out on related systems have shown remarkable agreement between the vacuum decay obtained from TWA and bubble nucleation obtained from the instanton approach [4–8]. We therefore proceed to compare the two approaches in the spin-1 system.

We take a one dimensional system with periodic boundary conditions, such as would be seen in an ultracold atom ring trap. Including the projector, the dimensionless PGPE reads

$$i \frac{\partial\psi}{\partial t} = \mathcal{P} \left\{ -\frac{1}{2} \frac{\partial^2\psi}{\partial x^2} + \frac{\partial V}{\partial\psi} \right\}, \quad (12)$$

In order to represent the quantum fluctuations, we take a stochastic field  $\psi$  initially in the false vacuum state with small fluctuations correlated to match the linearised quantum system. Most of the fluctuations are in the Bogliubov modes corresponding to the phase direction, and we have placed the noise in these modes only. The relevant sector of Bogliubov-de Gennes modes has dispersion relation

$$\omega(k) = \frac{1}{2} \left( k^2 + 2\omega_q \right)^{1/2} \left( k^2 + m_\varphi^2 \right)^{1/2}, \quad (13)$$

and the fluctuations associated with these modes has power spectrum

$$\langle \varphi_k \varphi_{k'} \rangle = \frac{1}{8\rho\zeta^2} \left( \frac{k^2 + 2\omega_q}{k^2 + m_\varphi^2} \right)^{1/2} \delta_{kk'} \quad (14)$$

This is identical to a Klein-Gordon result in the range  $k \ll (2\omega_q)^{1/2}$ . When combined with limits on the quadratic Zeeman shift in the BA vacuum, fluctuations will appear relativistic when  $k \ll 2|g'/g|^{1/2}$ . It follows that it is more difficult to replicate relativistic behaviour in systems with very small values of  $|g'/g|$ .

The projection  $\mathcal{P}$  in the PGPE cuts off modes with wave number  $k > k_c/2$ , where  $k_c$  is the largest wave number that can be accommodated on the finite sized grid, ensuring we can compute the time-evolution of the field using a Fourier pseudospectral method without any aliasing of the nonlinear terms. In our simulations we use a 601-point grid of length  $120\xi$ , and evolve the equations with a 4th order Runge–Kutta timestep of  $dt = 10^{-4} \omega_0^{-1}$  using XMDS2 software [17]. To reduce the possible parameter space we fix the quadratic Zeeman shift to  $\omega_q = -2g'/3g$  in all simulations.

Our simulations show that the system nucleates false vacuum regions, as in the examples shown in Fig. 4. In this periodic simulation, single bubbles undergo self-collision. In the collision region, there is a sudden release of energy that locally restores the metastable state for a short while. The decay is measured by marking the time at which the spatial average  $\langle \cos \varphi \rangle$  becomes larger than  $-1 + \delta$ , where  $\delta = 0.9$  is chosen to be much larger than the typical fluctuations of  $\langle \cos \varphi \rangle$  due to quantum fluctuations in the system. Running many stochastic trajectories allows us to compute the probability,  $P$ , of remaining in the metastable state at time  $t$ . A fit to the exponential form  $P = ae^{-\Gamma t}$  over the time intervals seen to be exhibiting exponential decay (we find this to be times late enough that  $P < 0.7$ ) yields the decay rate  $\Gamma$ . The decay rates for two systems are plotted in Fig. 5, with error bars estimated using a bootstrap procedure as described in [18]. The decay rates have also been compared to the prediction using Coleman’s instanton method,  $\Gamma = ABe^{-B}$ , using values for the exponent  $B \equiv B(\rho, \lambda)$  taken from [19]. In common with our previous work [12], we found it necessary to modify the effective value of the coupling and replace it with a renormalised value  $\lambda_{\text{eff}}$ . Treating the prefactor  $A$  and the coupling  $\lambda$  as free parameters in the fit is an interim measure that could be improved if the radiative corrections to the tunnelling exponent were known.

Finally, we comment on the experimental viability of our system. We tabulate relevant physical properties for alkali species with the required property  $g'/g < 0$  in Table I. The ground state hyperfine energy splitting  $\Delta E_{\text{hfs}}$  determines the magnetic field needed to achieve a given quadratic Zeeman shift [15]. While  $g'/g$  is fixed by the atomic species, there is considerable flexibility in choosing tunable experimental parameters that correspond to the dimensionless parameters used in our simulations. As examples, the parameters used in Figs. 4 and 5 (a) with  $\rho\xi = 20$  would correspond to 2400  $^7\text{Li}$  atoms in a 260  $\mu\text{m}$  circumference ring trap with transverse frequency  $\omega_r = 2\pi \times 25$  kHz and a bias field of  $B_z = 0.39$  Gauss. The timescale  $\omega_0^{-1}$  corresponds to 0.52 ms. The parameters used in Fig. 5 (b) with  $\rho\xi = 7$  would correspond to 840  $^{41}\text{K}$  atoms in a 24.4  $\mu\text{m}$  circumference ring trap with the same transverse frequency and a bias field of  $B_z = 0.23$  Gauss. We assume there is very wide experimental flexibility in terms of the coupling field Rabi frequencies and detuning ( $\Omega$ ,  $\Omega_{\pm}$ ,  $\Delta$ ); in practice these would need to be tuned to give the desired  $\epsilon$  and  $\lambda$  by taking into account the additional, smaller,

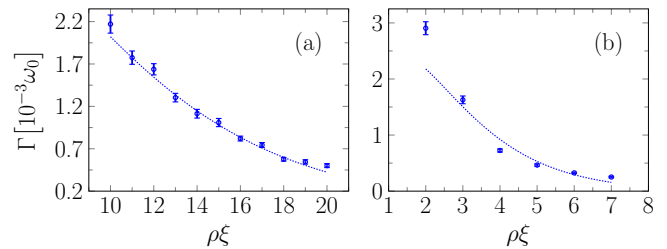


FIG. 5. The vacuum decay rate  $\Gamma$  for (a)  $^7\text{Li}$  and (b)  $^{41}\text{K}$ , with  $\lambda = 1.7$  and  $\epsilon = 0.05$ , plotted as a function of the particle density  $\rho$ . The solid curve represents the decay rate calculated using the instanton method, after fitting to the prefactor  $A$  and an effective coupling  $\lambda_{\text{eff}}$ . There is good agreement to the relativistic theory for  $^7\text{Li}$ , but less good agreement for  $^{41}\text{K}$  (which has a smaller value of  $|g'/g|$ ).

TABLE I. Physical properties used to compute simulation parameters. Scattering lengths are from the table in Ref. [15].

Species	$a_0$ ( $a_{\text{Bohr}}$ )	$a_2$ ( $a_{\text{Bohr}}$ )	$g'/g$	$\Delta E_{\text{hfs}}$ (MHz)
$^7\text{Li}$	23.9	6.9	-0.456	$803.5 \times h$ [20]
$^{41}\text{K}$	68.5	63.5	-0.0256	$254.0 \times h$ [21, 22]
$^{87}\text{Rb}$	101.8	100.4	-0.0046	$6834.7 \times h$ [23]

light shifts arising from the other states in the upper hyperfine manifold that we neglect here. We note that the example parameter values suggested above would appear to require a very low temperature (2.5 nK for  $^7\text{Li}$  and 16.6 nK for  $^{41}\text{K}$ ) to achieve complete phase coherence across the system in a single-component Bose gas. Crucially, however, the false vacuum state exists in the *relative* phase, and the relevant condition is that  $T < m_\varphi$  in dimensionless units. This sets the temperatures for *relative* phase coherence to 53 nK for  $^7\text{Li}$  and 352 nK for  $^{41}\text{K}$ . In principle, false vacuum decay should be observable in  $^{87}\text{Rb}$ , but we were unable to find a favourable parameter regime given the very small  $|g'/g|$  ratio.

In conclusion, we identified a metastable state of an effective Klein-Gordon field in a radio frequency and optical Raman coupled spin-1 Bose gas, which could serve as a laboratory example of false vacuum decay. Compared to previous proposals using same-species two-component Bose gases our proposal does not require time-modulation of the coupling, thus avoiding problematic instabilities, and avoids the need to minimize inter-component scattering length using Feshbach resonances. We numerically characterized false vacuum decay in the system, finding reasonable agreement with instanton predictions. Our proposal may provide a practical alternative system in which to realize an analogue to relativistic false vacuum decay in  $^7\text{Li}$  or  $^{41}\text{K}$  experiments.

Data supporting this publication are openly available under a Creative Commons CC-BY-4.0 License in Ref. [24].

**Acknowledgements:** We would like to thank Jonathan Braden for helpful discussions. This work was supported by the UK Quantum Technologies for Fundamental Physics programme [grant ST/T00584X/1]. KB is supported by an STFC

studentship. This research made use of the Rocket High Performance Computing service at Newcastle University.

---

\* [thomas.billam@ncl.ac.uk](mailto:thomas.billam@ncl.ac.uk)

† [k.brown@ncl.ac.uk](mailto:k.brown@ncl.ac.uk)

‡ [ian.moss@ncl.ac.uk](mailto:ian.moss@ncl.ac.uk)

- [1] S. R. Coleman, *Phys. Rev. D* **15**, 2929 (1977), [Erratum: *Phys. Rev. D* **16**, 1248 (1977)].
- [2] C. G. Callan and S. R. Coleman, *Phys. Rev. D* **16**, 1762 (1977).
- [3] S. R. Coleman and F. De Luccia, *Phys. Rev. D* **21**, 3305 (1980).
- [4] O. Fialko, B. Opanchuk, A. I. Sidorov, P. D. Drummond, and J. Brand, *EPL (Europhysics Letters)* **110**, 56001 (2015), [arXiv:1408.1163](https://arxiv.org/abs/1408.1163) [cond-mat.quant-gas].
- [5] O. Fialko, B. Opanchuk, A. I. Sidorov, P. D. Drummond, and J. Brand, *Journal of Physics B Atomic Molecular Physics* **50**, 024003 (2017), [arXiv:1607.01460](https://arxiv.org/abs/1607.01460) [cond-mat.quant-gas].
- [6] J. Braden, M. C. Johnson, H. V. Peiris, and S. Weinfurter, *JHEP* **07**, 014 (2018), [arXiv:1712.02356](https://arxiv.org/abs/1712.02356) [hep-th].
- [7] J. Braden, M. C. Johnson, H. V. Peiris, A. Pontzen, and S. Weinfurter, *Phys. Rev. Lett.* **123**, 031601 (2019), [arXiv:1806.06069](https://arxiv.org/abs/1806.06069) [hep-th].
- [8] M. P. Hertzberg, F. Rompineve, and N. Shah, *Phys. Rev. D* **102**, 076003 (2020).
- [9] M. J. Steel, M. K. Olsen, L. I. Plimak, P. D. Drummond, S. M. Tan, M. J. Collett, D. F. Walls, and R. Graham, *Phys. Rev. A* **58**, 4824 (1998), [arXiv:cond-mat/9807349](https://arxiv.org/abs/cond-mat/9807349) [cond-mat.soft].
- [10] P. Blakie, A. Bradley, M. Davis, R. Ballagh, and C. Gardiner, *Advances in Physics* **57**, 363 (2008), [arXiv:0809.1487](https://arxiv.org/abs/0809.1487) [cond-mat.quant-gas].
- [11] J. Braden, M. C. Johnson, H. V. Peiris, A. Pontzen, and S. Weinfurter, *JHEP* **10**, 174 (2019), [arXiv:1904.07873](https://arxiv.org/abs/1904.07873) [hep-th].
- [12] T. P. Billam, K. Brown, and I. G. Moss, *Phys. Rev. A* **102**, 043324 (2020), [arXiv:2006.09820](https://arxiv.org/abs/2006.09820) [cond-mat.quant-gas].
- [13] K. C. Wright, L. S. Leslie, and N. P. Bigelow, *Phys. Rev. A* **78**, 053412 (2008).
- [14] Y. Kawaguchi and M. Ueda, *Physics Reports* **520**, 253 (2012), [arXiv:1001.2072](https://arxiv.org/abs/1001.2072) [cond-mat.quant-gas].
- [15] D. M. Stamper-Kurn and M. Ueda, *Rev. Mod. Phys.* **85**, 1191 (2013), [arXiv:1205.1888](https://arxiv.org/abs/1205.1888) [cond-mat.quant-gas].
- [16] M.-S. Chang, Q. Qin, W. Zhang, L. You, and M. S. Chapman, *Nature Physics* **1**, 111–116 (2005).
- [17] G. R. Dennis, J. J. Hope, and M. T. Johnsson, *Computer Physics Communications* **184**, 201 (2013), [arXiv:1204.4255](https://arxiv.org/abs/1204.4255) [physics.comp-ph].
- [18] T. P. Billam, R. Gregory, F. Michel, and I. G. Moss, *Phys. Rev. D* **100**, 065016 (2019), [arXiv:1811.09169](https://arxiv.org/abs/1811.09169) [hep-th].
- [19] M. Gutierrez Abed and I. G. Moss, [arXiv:2006.06289](https://arxiv.org/abs/2006.06289) [hep-th].
- [20] C. Foot, *Atomic Physics*, Oxford Master Series in Physics (OUP, Oxford, 2005).
- [21] S. Falke, E. Tiemann, C. Lisdat, H. Schnatz, and G. Grosche, *Phys. Rev. A* **74**, 032503 (2006).
- [22] E. Arimondo, M. Inguscio, and P. Violino, *Rev. Mod. Phys.* **49**, 31 (1977).
- [23] S. Bize, Y. Sortais, M. S. Santos, C. Mandache, A. Clairon, and C. Salomon, *Europhysics Letters (EPL)* **45**, 558 (1999).
- [24] T. P. Billam, K. Brown, and I. G. Moss, “False vacuum decay in an ultracold spin-1 Bose gas,” (2021), dataset available at [doi:10.25405/data.ncl.15097368](https://doi.org/10.25405/data.ncl.15097368).